Corrosion failure of post-tensioning tendons in alkaline and chloride-free segregated grout: a case study

Maddalena Carsana* and Luca Bertolini[1]

Department of Chemistry, Materials and Chemical Engineering "G. Natta", Politecnico di Milano, via Mancinelli 7, Milan 20131, Italy

(*Received 3 September 2013; final version received 29 November 2013; accepted 9 December 2013; published online 26 March 2014*)

1. Introduction

Cases of corrosion of tendons in post-tensioned structures due to incomplete filling of the ducts (i.e. lack of grout in contact with steel), penetration of chlorides through defects of the ducts or hydrogen embrittlement are well documented (Bertolini, Elsener, Pedeferri, Redaelli, & Polder, 2013; *fib*, 2005; Freyermuth, 1991; Henriksen, Knudsen, & Braestrup, 1998; Nagi & Whiting, 1996; Nürnberger, 2002; Nürnberger & Sawade, 2007; Schupack, 1978; Schupack, 1991; Szilard, 1969). Recently, cases of severe corrosion attacks on strands in contact with segregated grout have also been documented (Godart, 2001; Lecinq, 2004). This phenomenon was reported mainly in the highest parts of external post-tensioning tendons of box girder bridges, where a whitish unhardened paste was found in the ducts, characterised by an alkaline pH and high content of sulphate ions.

Corrosion attacks found in these areas were deep penetrating and, in some cases, led to the rupture of the tendons. Cases of failure of external post-tensioning tendons have also been reported for other bridges where segregation of grout occurred, although published details are scarce (Bricker & Shokker, 2005; Poston & West, 2001; Powers, Sagues, & Virmani, 2013; Suarez, Zhang, Hsuan, & Hartt, 2006; Texas Transportation Institute, 2013). Studies have been carried out in order to improve the stability of injection grouts, thus preventing segregation and related corrosion problems (Chaussin & Chabert, 2001; Poston & West, 2001), and recently specific tests were developed to assess the stability of the grout, which are now part of European standards (EN 445, 2007). Nevertheless, the corrosion mechanism that leads to heavy corrosion attack on steel strands embedded in the alkaline and non-chloride contaminated segregated grout is still unclear.

Unfortunately, in spite of the potential high structural risks associated to this corrosion phenomenon, there is lack of documentation of failures that could help in understanding the corrosion mechanism. This paper describes a case study of a bridge that experienced a complete failure of an external post-tensioning tendon and, then, was subjected to a thorough inspection, which included the replacement of several tendons. For the sake of disseminating the experience on this rather unknown corrosion phenomenon, results of the failure analysis that are not covered by confidentiality are described.

2. Bridge description

The bridge is a segmental box girder post-tensioned with external tendons consisting of 27 seven-wire high strength steel strands located inside grouted high-density polyethylene ducts. Spans of the bridge ranged from about 50 to 125 m. The ducts were injected with a grout mixed at the construction site with water/cement ratio 0.32 and the addition of a commercial admixture specific for grouts. The fresh grout was able to pass the inclined-tube test and the wick test according to EN 446 standard and thus was considered potentially able to fill the ducts without segregating.

*Corresponding author. Email: maddalena.carsana@polimi.it

Rupture of one of the external tendons was detected after less than 2 years from the construction. Deep localised corrosion attacks, with a morphology similar to that usually occurring as a consequence of chloride-induced pitting attacks (Bertolini, 2008), were clearly observed at the naked eye on the wires of the strands. Corrosion was associated to the presence of a segregated whitish unhardened paste. The reasons for segregation could not be assessed. A detailed inspection of this bridge was carried out after the discovery of the failure of the post-tensioning tendon. Investigations were carried out on the tendon that failed under service as well on the other tendons, some of which were removed in order to carry out a thorough investigation of the grout and the embedded steel strands. Laboratory analyses were carried out on grout and steel samples collected in different representative locations of the tendons.

3. Analysis of the tendon failed in service

Two segments of the failed tendon were brought to the laboratory for inspection, i.e. a portion near one of the anchor head where the tendon failed, and a further portion that was near to the failure zone, but the injection grout was still present inside the duct (Figure 1). The visual observation of the failed strands near the anchor head (Figure 1(a)) showed the presence of corrosion products and many localised attacks (Figure 1(b)). This phenomenon occurred mainly in the parts where residues of a whitish unhardened paste were found on the surface of the steel (Figure 1(c)). All the corrosion attacks were localised, some of which were shallow while others were very penetrating. Localised attacks initiated preferentially at the regions of contact between the wires (Figure 2).

In order to estimate the reduction of cross section of the tendon induced by corrosion before the failure, the wires of the strands still anchored to the anchor head (Figure 1(a)) were analysed individually. Two complete strands as well as the central wire of several other strands were no more present (probably they were removed during the rupture of the tendon), so that about 24% of the expected wires were missing. Each of the remaining wires was visually observed in order to identify the type of rupture, the location of the break (i.e. distance from the

Figure 1. Portions of the failed tendon analysed in the laboratory.

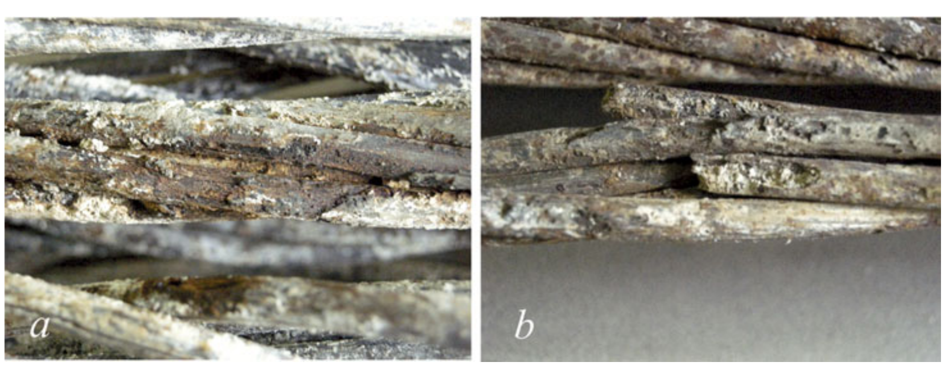

Figure 2. Examples of corrosion attacks observed on the surface of the strands.

head), and the extent and depth of corrosion attacks. Corrosion attacks were randomly distributed along the length of inspected portion of the tendon. The rupture was classified as: C when most of the cross section was depleted by the corrosion, N when a clear ductile necking failure was observed and NC when a mix of corrosion and ductile final failure occurred. Figure 3 shows examples of the three types of failure.

Figure 4 shows that about 15% of the wires had the cross section mainly consumed by corrosion attacks and, therefore, it may be assumed that they failed before the rupture of the tendon. Furthermore, for slightly more than 30% of the remaining wires, fracture may be attributed to partial corrosion (type NC). Wires that have undergone only necking and those that are missing constitute 53.4%of the total; for these wire, it is reasonable to assume that the cross section was essentially undamaged at the time of failure. Assuming, in the first approximation, that the condition for NC can be considered on average as a reduction of cross section due to corrosion of 50%, it may be estimated that the reduction in the whole cross section of the tendon due to corrosion attack occurred before the final failure was approximately 30%. Such a value can justify the collapse under service, taking into account that the post-tensioning force was equivalent to about 75% of the tensile stress of the steel.

Figure 3. Examples of the types of failure observed on the wires of the tendon failed in service.

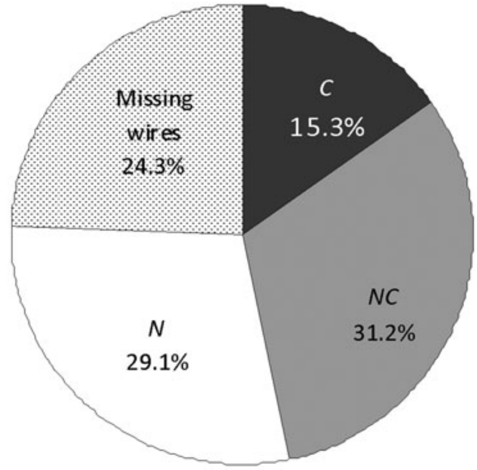

Figure 4. Summary of the types of failure (C, corrosion; N, necking; NC, corrosion + necking) observed on the wires of the tendon failed in service.

The second portion of the tendon that was inspected in the laboratory consisted of a first section of naked strands (about 3.0 m long) and a second portion (of about 2.3 m) in which the strands were still embedded in the grouted duct (Figure 1(d)). A length of about 60 cm of the latter part was opened (Figure 1(e)) in order to evaluate the degree of filling and observe the surface the embedded steel wires. Although this section of the tendon was completely filled, the filling grout was non-homogeneous. Three different areas were distinguished (Figure 1(f)): (1) a zone with a grey hardened cement paste in the bottom part, (2) an intermediate part with a whitish friable material and (3) an upper part with a whitish and damp paste, with a plastic consistency (after about 24 h from the aperture of the duct, this latter paste dried out and become friable like in the intermediate zone). Shallow corrosion attacks were observed on 12 of the 27 strands, particularly on those in contact with the whitish substance.

Subsequently, the rest of the portions of tendon shown in Figure 1(d) were inspected and, besides the hardened grey paste and the unhardened whitish paste, two further types of hardened grout were observed (presumably formed as a result of segregation). The first type, which appeared at the naked eye as a light grey hardened paste with small black spots, was found between the whitish paste and the grey hardened paste. Shallow corrosion attacks were occasionally observed on steel embedded in this type of grout. A further type of grout had a dark grey colour and was located in the portion of the duct which presumably corresponded to the bottom part under service. No corrosion attacks were observed on steel wires embedded in the grey and dark grey grout.

The remaining parts of the tendon failed under service were inspected at the bridge site, by observing the cross section in correspondence of cuts produced at lengths of about 6–7 m to allow the removal of the tendon from the bridge. In the cut surfaces far from the anchor head, only the hardened grey grout and, occasionally, the dark grey grout on the bottom were observed.

4. Inspection of tendons still in service

To gather information on the conservation state of the other tendons of the bridge, in the inclined part between the last deviation point and the anchorage at both ends of each tendon, the duct was removed for a length of about 0.5 m (Figure 5). These apertures allowed the visual observation of the filling of the duct, the surface of the grout previously in contact with the duct and the steel wires which were either not embedded in the grout or visible on the surface of the grout. Some apertures on the opposite side to the injection point were expanded to a length of about 3 m. Although in most cases the ducts were filled with hardened grout of a regular aspect, also grout with consistency and colour similar to that found in the tendon failed in service could be observed.

Figure 6 depicts the different aspect of the filling material found in the inspected tendons. On the basis of the observation of more of 60 samples, collected during the inspection of the tendon failed in service and of tendons removed afterwards, the consistency and the colour of the grout were detected and the filling material was classified as follows: G = hardened grout with a regular aspect and the typical grey colour; B = hardened grout with a dark grey (almost black) colour; W = unhardened whitish grout (i.e. in the form of a plastic paste, if wet, or a weak and friable material, if dry); P = light grey coloured hardened grout with black spots. As a general trend, types G and B were found at the bottom of the duct, type W on the top and P at an intermediate position. Voids (V) were also found in some cases in the upper part of the duct.

Figure 5. Example of an aperture in the duct of a tendon showing the whitish segregated grout embedding corroding strands.

Figure 7 summarises the results of the inspections on the apertures, showing the percentage of tendons where the different types of grout were detected along the surface previously in contact with removed ducts. Data have been analysed separately for the apertures of the injection side (Figure 7(a)) and in the opposite side (Figure 7(b)) of the five spans (A–E) of the bridge. These graphs, while representing the results of a simplified analysis, which is subjective and limited to visual observation of the surface exposed after partial removal of the duct, show the coexistence of different types of grout in the tendons of the spans of the bridge.

Furthermore, it can be seen that the presence of W grout was higher in the side opposite to that of injection. In most cases, only traces of this grout were observed (usually in the form of a thin stripe on the top of the duct), but in few cases a remarkable amount of W grout was detected and embedded strands were covered by corrosion products or even showed localised attacks. Grout P could be rarely detected from the surface.

In correspondence of the apertures, the alkalinity of the grout was evaluated by means of a commercial pH indicator, which always revealed a pH value in the upper range (≥ 13), regardless of the colour and consistency of the grout. Nonetheless, corrosion products were detected

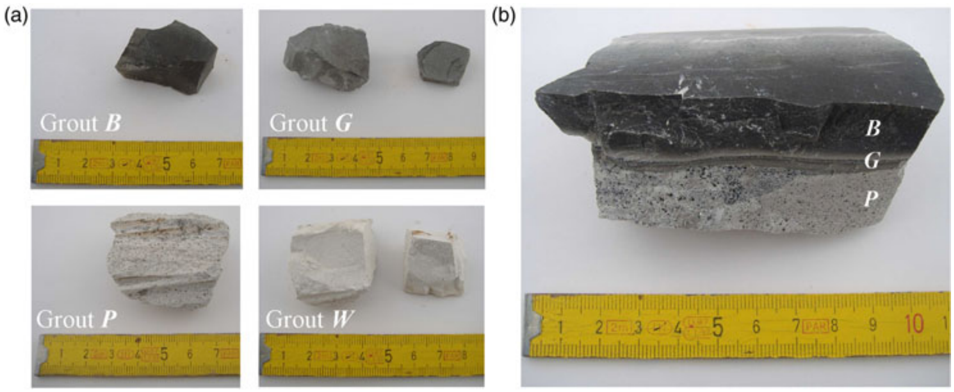

Figure 6. Different types of aspect of grout collected from the removed ducts of the inspected tendons (a) and example of stratification of the grout after segregation (b).

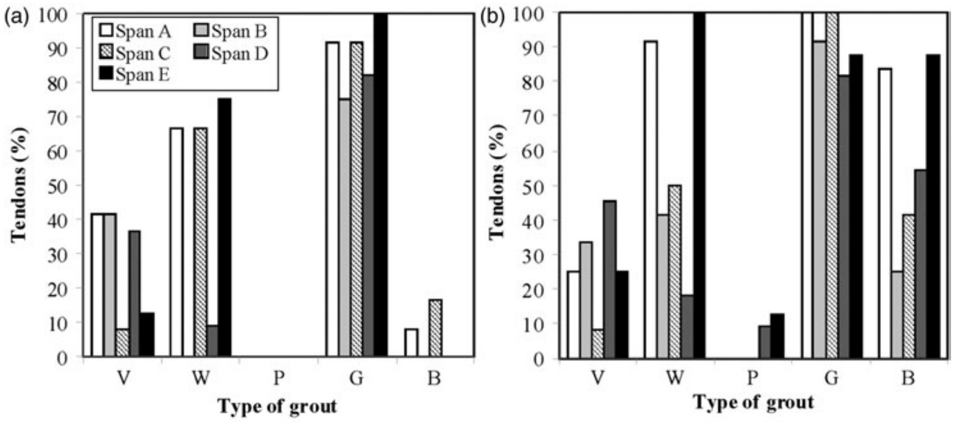

Figure 7. Percentage of tendons showing the presence (even only in traces) of the different types of grout (V, voids; W, unhardened whitish grout; P, light grey grout; G, grey hydrated grout; B, dark grey grout) in the apertures on the inclined parts of the injection side (a) and the opposite side (b).

on the surface of the strands that emerged from grout W (Figure 5), in few cases also deep penetrating attacks could be observed.

In order to further investigate the corrosion phenomenon, six tendons (conventionally named a–f) that showed during the inspection of the apertures penetrating corrosion attacks and/or a significant amount of grouts W or P were removed for inspection and replaced. For the practical necessity of extracting the tendons from the viaduct, they were cut in segments that were inspected outside the bridge (Figure 8). Each cutting section was observed in order to detect the presence of different types of grout along the length of the tendon (Figure 8(a)). Then, in the two external segments with the anchor heads, the polyethylene duct was removed and the corrosion potential of steel strands was measured versus a $Cu/CuSO_4$ reference electrode (Figure 8(b)) before the grout could dry out. The filling material was observed in order to document the types of grout and their position and to collect samples for laboratory analysis (Figure 8(c)), and

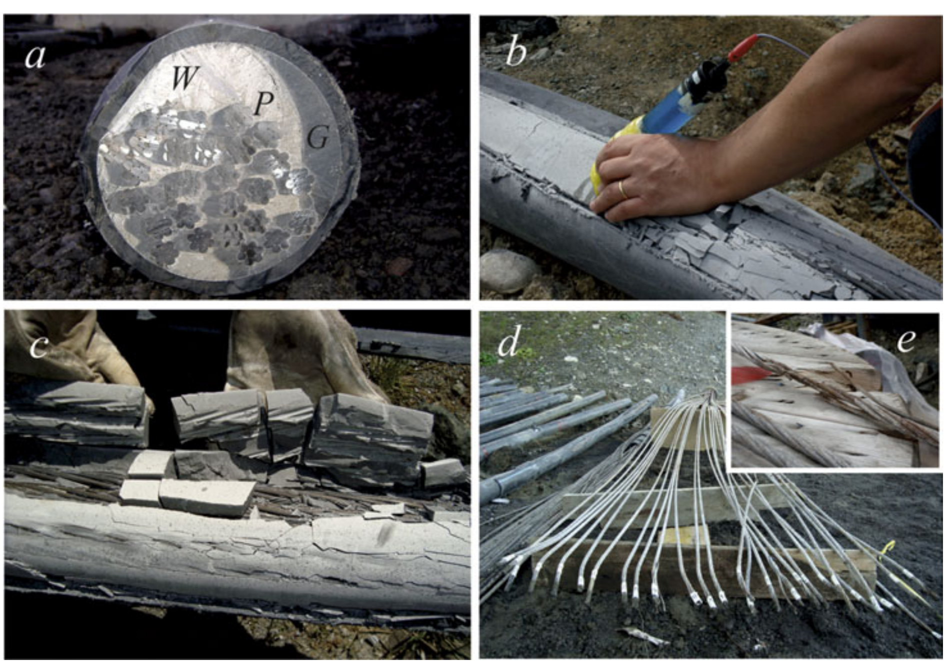

Figure 8. Inspection of a tendon removed from the bridge: (a) types of grout observed on a cutting section, (b) measurement of the corrosion potential of steel strands, (c) inspection of the grout, (d) inspection of the steel strands and (e) detail of wires of a strand broken due to corrosion.

thereafter each single strand was removed and carefully checked (Figure 8(d)) to detect the presence of broken wires and corrosion attacks (Figure 8(e)).

Table 1 summarises the observations made on the tendons removed from different spans of the bridge, by comparing the results of the analyses carried out after the removal of the tendon with the results of the previous visual observation from the apertures in the ducts. The detailed inspection of the portion of the tendons near the anchor heads confirmed the presence of penetrating corrosion attacks, which in some cases led to breaking of several wires. Localised corrosion was always associated to the presence of the type W grout or, to a lesser extent, to the type P grout. Table 1 shows that, apart one case, such attacks were found only in the inclined part of the tendons opposite to the side of injection. No broken wires were found at the injection side and the number of strands with penetrating corrosion attacks (with depth higher than 1 mm, visible at the naked eye) was negligible. No corrosion attacks were found in the areas where the strands were embedded in a regular hardened cement grout (i.e. type G) or with dark grey grout (type B).

In order to verify the reliability of the visual inspection from the apertures in the ducts, further four tendons (named g –i, Table 1) were removed, which were randomly selected between the remaining tendons that showed only negligible traces of whitish paste and did not show corrosion attacks on the steel strands visible from the apertures. These tendons were thoroughly inspected along the whole length. Figure 9 summarises the results of the inspection made on one of these tendons. Figure 9(a) shows the 18 portions in which the tendon was cut (the symbol + indicates the position of cutting), the type of grout detected in each segment (identified through the corresponding letter, as previously defined) and the degree of filling observed in correspondence of each cutting section (quantified on the *y*-axis by the filled symbols).

The filling was complete, except for the end portions with the anchor heads (#1 and #18), where, however, the grout was ejected as a result of the damage occurred during the removal operations. In all the other portions, only type G grout was found. Grout samples were collected from each segment of the tendon to measure the moisture content and the water absorption (Figure 9(b)). The moisture content of the grout at the time of sampling approached the absorption of the sample (equal to about 20% by mass, Figure 9(b)), i.e. the grout along the duct was still saturated with water. Figure 9(c) shows the results of the observation of the 27 strands along the length of the tendon, showing that most of the surface of the steel was in passive conditions, and only few attacks with a penetration depth lower than 0.5 mm were observed on one strand near an anchorage. Figure 9(d) shows that the corrosion potential of the steel embedded in the grout was in the range of $-250/-200$ mV versus $Cu/CuSO_4$ along the tendon.

The potential measurements, which were carried out immediately after the removal of the duct, showed that this technique is not able to detect those areas in which small localised attacks were present. Measured potential values were those typical of passive areas in water-saturated grout (Bertolini et al., 2013), while lower values of corrosion potential that are expected in the neighbourhood of localised attacks could not be detected by the reference electrode placed on the external surface of the grout.

Detailed inspection of tendons g–i showed that steel strands were passive along the full length. No broken wires were found (Table 1), and only some tiny and shallow corrosion attacks were observed on few wires in contact with traces of W grouts near the anchorages of tendons g

Table 1. Summary of the inspection on the portions with the anchor heads of the tendons that were removed and inspected, and comparison with the results of the previous observation from the apertures in the duct.

	Broken wires		Strands with corrosion attacks[a]		Visual observation from the apertures in the duct[b]			
Tendon	Side opposite to injection	Injection side	Side opposite to injection (%)	Injection side (%)	V	W	P	C
a	10	–	63	–	✓	✓		✓
b	5	–	81	–	✓	✓		✓
c	21	0	44	33	✓	✓		✓
d	0	0	52	0	✓	✓		✓
e	11	0	41	0	✓	✓		✓
f	9	0	54	0	✓	✓	✓	✓
g	0	0	7	0	✓	✓		
h	0	0	0	0		✓		
k	0	0	0	0		✓		
i	0	0	0	22	✓	✓		

[a] Percentage of strands that, during the inspection after the removal of the tendon, showed at least one corrosion attack with a penetration depth of 1 mm or higher along their length.
[b] V, voids (lack of filling grout); W, unhardened whitish grout (even only traces); P, light grey grout; C, corrosion traces on emerging steel wires.

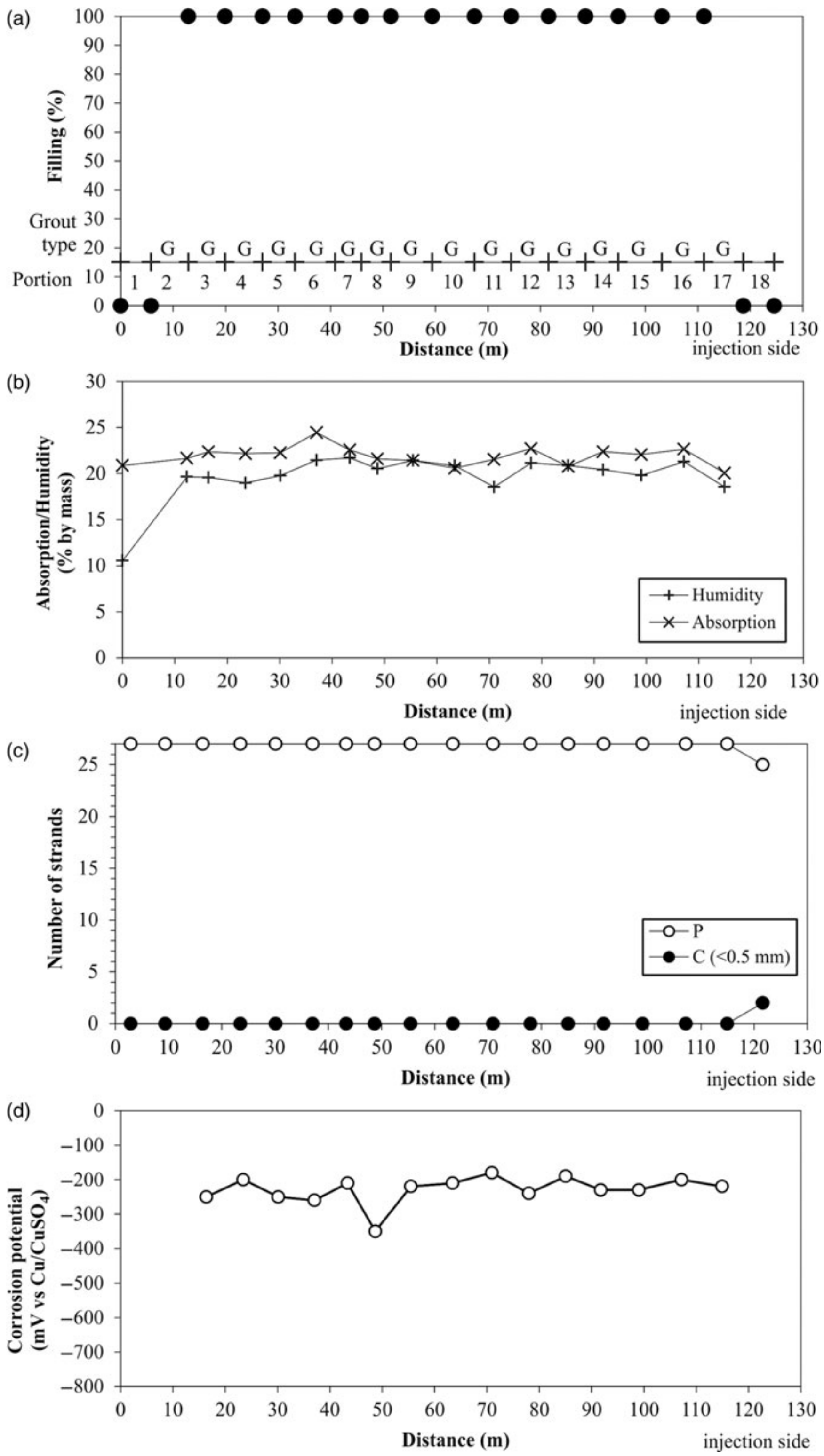

Figure 9. Example of the results of inspection of a tendon: (a) filling degree and types of grout observed on the cut sections, (b) moisture content and water absorption of grout specimens taken from different segments, (c) number of passive wires (P) and corrosion attacks (C) and (d) corrosion potential of the steel strands.

and i. These results confirm that no corrosion took place on steel embedded in G or B grouts and suggest that the observation from the apertures in the inclined part of the duct was able to detect the presence of significant amounts of segregated grout and thus the risk of corrosion of steel.

5. Laboratory analyses

Samples of different types of grout and steel strands were collected both from the tendon failed in service and the tendons that were removed afterwards, in order to be analysed in the laboratory.

5.1 Strands

Chemical analysis measured on a sample of steel wire is shown in Table 2, while the microstructure is shown in Figure 10. The surface of the corroded wires often shows the presence of significant amounts of corrosion products, which often have a brownish colour but, in some cases, also with a blackish colour. The presence of blackish corrosion products suggests that the corrosion attack propagated under conditions of lack of oxygen. X-ray diffraction analyses identified the presence of calcite ($CaCO_3$), ettringite ($Ca_6Al_2(SO_4)_3(OH)_{12}\cdot 26H_2O$), goethite (FeO (OH)) and magnetite (Fe_3O_4) in brownish corrosion products, and goethite and magnetite in the blackish ones.

Corroded areas and fracture surfaces of representative samples of steel wires were observed. Figure 11(a), for example, shows the failure of a wire, which took place in correspondence of a localised corrosion attack. Figure 10 shows the thick layers of flaky corrosion products observed on metallographic sections. At the scanning electron microscope (SEM), the fracture surface, where it was not masked by corrosion products, was ductile and characterised by the presence of elongated dimples (Figure 11(b)).

Wires failed due to corrosion, both in the tendon failed in service and in the tendons removed afterwards, were accurately observed in order to investigate on the possible presence of hydrogen-induced stress corrosion cracks. The presence of this form of attack was, however, excluded

Table 2. Chemical composition of the steel (% by mass).

C	Mn	Si	P	S	Cr	Ni	Mo	Al	Cu
0.81	0.88	0.18	0.008	0.013	0.14	0.047	0.014	0.003	0.028

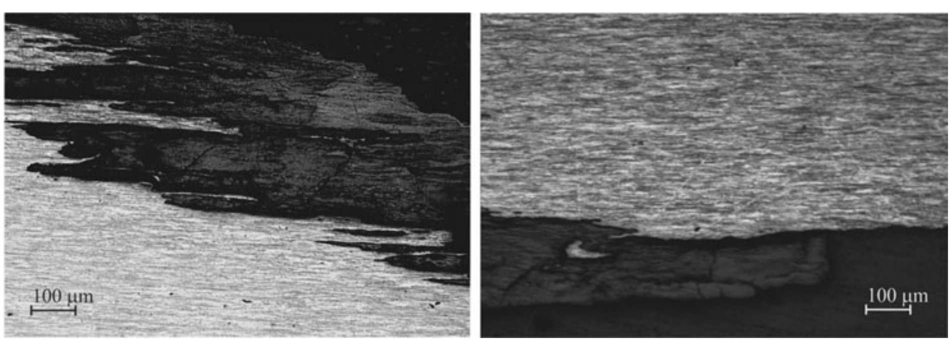

Figure 10. Metallographic sections of corroded wires from the tendons failed under service.

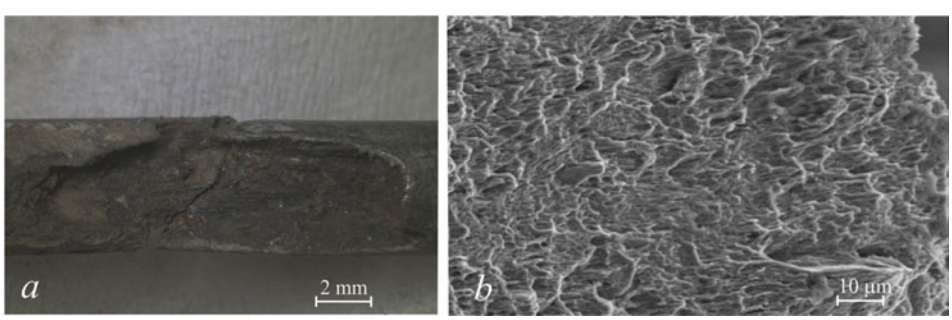

Figure 11. Stereomicroscope image of the two parts of a broken wire (a) and SEM image of the ductile fracture surface (b).

Table 3. Chemical composition (% vs dry mass) of grout, measured by ICP-OES analysis (average values) (Carsana & Bertolini, 2014).

Type of grout	K_2O	Na_2O	SO_3
W	1.61	1.11	6.29
P	1.13	0.69	3.12
G	0.55	0.42	2.66
B	0.35	0.32	1.85

for the following reasons: (a) the presence of abundant corrosion products on the metal surface, which suggests that corrosion is produced by a dissolution process rather than propagation of cracks; (b) the absence of any brittle fracture surface (only ductile fracture surface could be observed in areas not covered by corrosion products) and (c) the absence of any secondary cracks (typical of the propagation of hydrogen embrittlement) on the external surface of the wires.

5.2 Grout

Samples of the different types of grouts that were collected from the tendons were analysed by thermogravimetric analysis (TGA) and differential thermal analysis (DTA), physicochemical tests and scanning electron microscopy. Results of these analyses will be described in detail elsewhere (Carsana & Bertolini, 2014), while here only the main findings are summarised. Grout G (not segregated) was found to be a common hardened cement paste. Grout W, while being formed by the compounds normally present in the products of hydration of cement pastes, was characterised by a high content of soluble substances that form in the early stages of hydration of Portland cement.

Chemical analyses (Table 3) showed very high values of alkalis (Na_2O and K_2O, respectively, equal to 1.1% and 1.6% by mass) and sulphate ions (6.3%) in grout W. The presence of this grout, localised in correspondence of the highest parts of the duct and especially at the end opposite to that of injection, should be attributed to the segregation of the grout during the injection or in the early stage of hydration. Grout G had values of alkalis and sulphate ions in the expected range for hydrated cement paste, i.e. much lower than those found not only in the case of grout W but also in the case of grout P. Grout B, which was found in the lowest parts of the ducts, was characterised by the lowest values of alkalis and sulphates. The total chloride content (acid soluble) was negligible in all types of grout.

6. Conclusions

The failure of an external post-tensioning tendon of a bridge, which was detected after less than 2 years from the construction, was induced by the presence of deep localised corrosion attacks which were found in places where the injection grout had a whitish colour and appeared as a plastic (unhardened) paste, while after drying out it became incoherent and dusty.

A thorough investigation of all the post-tensioning tendons was carried out. An aperture was made in the duct in the inclined parts of the tendons near the anchorages. The whitish unhardened grout was found in traces in most of the tendons, while in few tendons it was present in significant amounts, which were associated to heavy corrosion attacks on the embedded strands. This whitish paste was identified as the result of segregation of the injected grout. Sometimes the segregated grout also had a light grey colour with small black spots and was hardened, although weak; this type of grout was observed in intermediate position between the regular grey hardened and the whitish grout. A dark grey type of grout was also found occasionally at the bottom of the duct.

Tendons showing corrosion attacks were removed and wires of the tendons were inspected, together with the tendon failed in service. It was confirmed that penetrating localised corrosion attacks only took place in the inclined part of the tendons near the anchorages, when the steel was embedded in the segregated grout. In this cases, extremely localised and deep attack could be observed, which also led to failure of some wires. Corrosion was due to dissolution and no cracks could be observed (which would be present in the case of stress corrosion cracking).

Corrosion rates of the order of several millimetres per year could be estimated, taking into account that in some cases the whole cross section of a wire was depleted in less than 2 years. Four tendons showing only traces of unhardened whitish grout in the apertures of the duct were also removed and inspected. In these cases, in accordance with the previous visual observation from the apertures in the duct, no significant amount of whitish paste along the full length of the tendon was detected and steel strands were found passive (apart from few cases showing tiny shallow attacks).

The case study described in this work confirms the serious risks associated to the segregation of the protection grout in external post-tensioning tendons and the importance of preventing this phenomenon by means of appropriate materials and procedures. Nevertheless, it also highlights the need for a better understanding of the corrosion phenomenon that takes place under these circumstances and its possible evolution in time. Indeed, due to the high pH of the segregated grout and the absence of chloride ions, the usual causes of steel corrosion in concrete cannot be responsible of the corrosion attacks.

Clearly, corrosion cannot be ascribed to carbonation, because of the alkaline nature of the segregated grout as well as the extremely localised morphology of the corrosion attacks. On the other hand, the absence of appreciable amounts of chloride ions in the grout allows to exclude the occurrence of chloride-induced corrosion. Furthermore, stress corrosion cracking phenomena (e.g. due to hydrogen embrittlement) and even the presence of stray current inside the plastic ducts have to be excluded. A possible mechanism for this corrosion phenomenon has been proposed by the authors (Bertolini & Carsana, 2011), suggesting that conditions of low availability of oxygen that may be produced in the interstices among wires of the strands can be responsible for the corrosion initiation, while the subsequent high rate of propagation of the attack can be ascribed to the macrocells that generates in the highly electrically conductive whitish paste between the small depassivated areas and the surrounding passive areas of the steel.

Acknowledgements

The authors are grateful to F. Brunella, N. Goffi, M. Ormellese and F. Traisci for their contribution to the tests.

Note

1. Email: luca.bertolini@polimi.it

References

Bertolini, L. (2008). Steel corrosion and service life of reinforced concrete structures. *Structure and Infrastructure Engineering*, *4*, 123–137.

Bertolini, L., & Carsana, M. (2011). High pH corrosion of prestressing steel in segregated grout. In C. Andrade & G. Mancini (Eds.), *Modelling of corroding concrete structures* (pp. 147–158). Dordrecht: Rilem Publications, Springer.

Bertolini, L., Elsener, B., Pedeferri, P., Redaelli, E., & Polder, R. (2013). *Corrosion of steel in concrete – Prevention, diagnosis, repair* (2nd ed.). Weinheim: Wiley-VCH.

Bricker, M.D., & Shokker, A.J. (2005). *Corrosion from bleed water in grouted post-tensioned tendons*. Skokie: Portland Cement Association.

Carsana, M., & Bertolini, L. (2014). Characterization of segregated grout promoting corrosion of post-tensioning tendons. submitted.

Chaussin, R., & Chabert, A. (2001). Strategies for improvement – Approach in France. In fib *Bulletin 15: Durability of post-tensioning tendons* (pp. 235–244).

EN 445 (2007). EN 445 Grout for prestressing tendons – Test methods. *European Committee for Standardization*.

fib (2005). *Durability of post-tensioning tendons*. *fib* Bulletin No. 33, Lausanne.

Freyermuth, C.L. (1991). Durability of post-tensioned prestressed concrete structures – An overview of research and experience. *Concrete International*, *13*, 58–65.

Godart, B. (2001). Status of durability of post-tensioned tendons in France. In fib *Bulletin 15: Durability of post-tensioning tendons* (pp. 25–42).

Henriksen, C.F., Knudsen, A., & Braestrup, M.W. (1998). Cable corrosion: Indetected. *Concrete International*, *20*, 59–72.

Lecinq, B. (2004). Recent research in France for the improvement of cement grouting. In *Proceedings of 2nd workshop on durability of post-tensioning tendons*. Zürich: ETH.

Nagi, N., & Whiting, D. (1996). Corrosion of prestressed reinforcing steel in concrete bridges: State-of-the-art. *ACI Special Publication SP*, 151–152.

Nürnberger, U. (2002). Corrosion induced failure mechanism of prestressing steel. *Materials and Corrosion*, *53*, 591–601.

Nurnberger, U., & Sawade, G. (2007). Degradation of prestressed steel. In C.L. Page & M.M. Page (Eds.), *Durability of concrete and cement composites* (pp. 187–246). Cambridge: Woodhead Publishing.

Poston, R.W., & West, J.S. (2001). North American strategies for improving bonded post-tensioned concrete construction. In fib *Bulletin 15: Durability of post-tensioning tendons* (pp. 245–255).

Powers, R.G., Sagues, A.A., & Virmani, Y.P. (2013). Corrosion of post-tensioned tendons in Florida bridges. (Research Report No. FL/DOT/SMO/04-475). Florida Department of Transportation. Retrieved February 28, 2013, from www.dot.state.fl.us

Schupack, M. (1978). A survey on the durability performance of post-tensioning tendons. *ACI Journal*, *75*, 501–510.

Schupack, M. (1991). Corrosion Protection for unbonded tendons. *Concrete International*, *88*, 51–57.

Suarez, J., Zhang, J., Hsuan, G., & Hartt, W. (2006). Polyethylene duct cracking on post-tensioning tendons in Florida segmented bridges. *ASCE Journal of Materials in Civil Engineering*, *18*, 581–587.

Szilard, R. (1969). Corrosion and corrosion protection of tendons in prestressed concrete bridges. *ACI Journal*, *66*, 42–59.

Texas Transportation Institute (2013). Effect of voids in grouted post-tensioned concrete bridge construction. (Report 0-4588-1). Retrieved February 28, 2013, from http://tti.tamu.edu/documents/0-4588-1-Vol1.pdf